Available online at www.sciencedirect.com
ScienceDirect
Journal of Sound and Vibration 303 (2007) 814–831
JOURNAL OF SOUND AND VIBRATION
www.elsevier.com/locate/jsvi

Robust estimation of coupling loss factors from finite element analysis

A.N. Thite*, B.R. Mace

Dynamics Group, Institute of Sound and Vibration Research, University of Southampton, Southampton SO17 1BJ, UK

Received 30 June 2006; received in revised form 15 December 2006; accepted 5 February 2007
Available online 6 April 2007

Abstract

There are well-established techniques by which the coupling loss factors (CLFs) of statistical energy analysis (SEA) can be estimated from finite element analysis (FEA). These are typically based on a single, selected system. A slightly different choice of system would give different estimates. There is a need for robust methods that give good estimates of the SEA average CLFs, independent of the details of the chosen system. Estimates of variance, confidence limits, are also of interest. Two approaches to this problem are discussed. These involve attempts to randomise the properties of the system and averaging the resulting estimates, but without repeating the full FEA. The first involves perturbation of component modal properties which can be related to perturbations in the modes of the assembled structure and hence to the energies and CLFs. In the second approach, it is assumed that the statistics of the modal properties of the system analysed are a fair representation, when taken over a wide enough frequency range, of the statistics of the modes of the SEA ensemble. The modes of the system are then randomly sampled to provide robust estimates. Numerical examples are presented. The methods are computationally very cheap.

1. Introduction

Energy based modelling approaches are often used to describe high-frequency vibrational behaviour of complex structures in some average or approximate way. The most important of these is statistical energy analysis (SEA) [1]. It provides a statistical approach to modelling physical systems, which share gross characteristics but whose properties differ in detail.

In SEA, the structure is divided into subsystems and the response is described in terms of the total time average subsystem energies $\mathbf{E}$ and input powers $\mathbf{P}_{\text{in}}$. These are, in principle, averages taken over an ensemble of structures whose properties differ in detail and, in practice, are also frequency averages. In an SEA model, these powers and energies are related by

$$\mathbf{P}_{\text{in}} = \mathbf{L}\mathbf{E}, \tag{1}$$

*Corresponding author. Tel.: +44 23 8059 3756; fax: +44 23 8059 3190.
E-mail address: ant@isvr.soton.ac.uk (A.N. Thite).

0022-460X/$ - see front matter © 2007 Elsevier Ltd. All rights reserved.
doi:10.1016/j.jsv.2007.02.004

where

$$\mathbf{L} = \omega \operatorname{diag}(\eta_j) + \omega \begin{bmatrix} \eta_{12} + \eta_{13} + \cdots & -\eta_{21} & \cdots \\ -\eta_{12} & \eta_{21} + \eta_{23} + \cdots & \cdots \\ \vdots & \vdots & \ddots \end{bmatrix} \tag{2}$$

is a matrix of damping (η_j) and coupling (η_{ij}) loss factors for subsystems i and j and ω is the centre frequency. To maintain energy conservation, the columns of the matrix of coupling loss factors (CLF) must sum to zero. The elements of $\mathbf{L}$ must also satisfy the consistency relation

$$n_i \eta_{ij} = n_j \eta_{ji}, \tag{3}$$

where n_i is the (asymptotic) modal density of subsystem i. For a system comprising two subsystems

$$\mathbf{L} = \omega \begin{bmatrix} \eta_1 + \eta_{12} & -\eta_{21} \\ -\eta_{12} & \eta_2 + \eta_{21} \end{bmatrix}. \tag{4}$$

Theoretical expressions exist for the CLFs for some circumstances, commonly using a wave approach [1]. Numerical estimates of the CLFs can be obtained from finite element analysis (FEA) of the system [2–6]. The process is essentially a numerical analogue of the power injection method (PIM) [7], which is often used to develop an experimental SEA model of a structure. It broadly involves the following steps: the system is modelled using FEA in a conventional manner, and the mass and stiffness matrices found; the modes of the system are determined; the point response to point, time-harmonic excitation is determined for "many" combinations of excitation and response points; these frequency responses are post-processed by averaging over a chosen frequency band and over the chosen excitation and response points. The result is a matrix of the so-called energy influence coefficients (EICs) $\mathbf{A}$, which relate the subsystem energies and input powers $\mathbf{E}$ and $\mathbf{P}_{\text{in}}$ by

$$\mathbf{E} = \mathbf{A}\mathbf{P}_{\text{in}}. \tag{5}$$

This matrix is then inverted to give

$$\mathbf{P}_{\text{in}} = \mathbf{X}\mathbf{E}; \quad \mathbf{X} = \mathbf{A}^{-1}. \tag{6}$$

Strictly, the SEA equations (1) relate *ensemble average* powers and energies, while the FE predictions $\mathbf{X}$ are based on a *single estimate* of frequency average quantities, which depend on the specific input data chosen for the FEA. Thus $\mathbf{X}$ is just an estimate of $\omega\mathbf{L}$, i.e.

$$\mathbf{X} = \omega\hat{\mathbf{L}}. \tag{7}$$

The CLF estimated from a single analysis is sometimes referred to as an *apparent coupling loss factor* (ACLF) [5] to distinguish it from ensemble based estimates. The estimated ACLFs differ from the CLFs for various reasons:

1. $\hat{\mathbf{L}}$ is found from FEA of a single, selected system, whereas $\mathbf{L}$ relates ensemble average powers and energies;
2. $\hat{\mathbf{L}}$ is found from averages over a finite, selected frequency band;
3. $\hat{\mathbf{L}}$ may be estimated using a finite number of excitation and response points, whereas $\mathbf{L}$ relates total subsystem energy for "rain-on-the-roof" excitation.

The first two reasons reflect the facts that there are only a few modes of the chosen system within the chosen finite frequency band, they may not represent the modes of the ensemble accurately, nor may they represent the modes of the chosen system over a broad frequency band: they are just a potentially small sample. The problem is exacerbated because estimating $\hat{\mathbf{L}}$ involves a matrix inversion, which can magnify errors if $\mathbf{A}$ is not well conditioned. Common experience and numerical studies have shown that the variability tends to be larger for lower modal overlap or if there are relatively few modes in the band [8–11]. (The modal overlap of the system is $M = n\Delta$, where Δ is the average half-power bandwidth.)

There is therefore an interest in robust estimation of the CLFs, i.e. estimates which do not depend sensitively on the properties of the specific system chosen for analysis, together with estimating variance or confidence limits for a single prediction. One approach might be to perform a Monte Carlo simulation (MCS) for a sample of systems with similar but different properties, to average the energies and input powers and then invert the resulting matrix **A**. This would require many FE calculations and would normally be time consuming and computationally expensive.

In this paper two approaches are suggested, with particular reference to the case of a system comprising just two subsystems. A single FEA is performed, but then the properties of the system are randomised and the resulting energies and powers averaged. The first approach involves component mode synthesis (CMS) and a perturbation in which the fixed interface subsystem natural frequencies are randomised. The method follows that of Mace and Shorter [12] for estimating frequency response statistics. In the second approach random samples are drawn from the modes of the system as calculated from the FEA. These give estimates for the "average" CLF, together with an indication of the variability of single estimates. Numerical examples are presented. Further details can be found in Ref. [13].

One issue that is not addressed is how the ensemble is defined. In practice this is likely to be case-dependent and problematical, with there being little practical evidence to justify a specific choice for the statistics of the subsystem properties across the ensemble. However, the detailed definition of the ensemble is not likely to be important if the variability is "large enough" [14–20]. In any event, including *some* randomness is likely to give better estimates of the mean than a single FEA estimate of the ACLFs. Also not considered is uncertainty in damping loss factor. This is unimportant for weak coupling where the CLFs are independent of damping. Whether this is the case or not will not be known *a priori*. However, it is straightforward to include variability in damping because the modal properties remain unchanged, so that MCS of the EICs only involves recalculation of the modal powers and modal sums. Finally, ideally the excitation is random, distributed "rain-on-the-roof". In some previous work, and in experimental SEA, this has been approximated by a number of discrete point forces and the energy approximated by an average of point responses giving two further sources of variability, but ones that can be avoided by suitable post-processing of the FEA [6].

In the next section, expressions for the EICs in terms of the modes of the system are reviewed, following [6,21,22]. The EICs depend on the system's natural frequencies and mode shapes. Sources of variability in the EICs and ACLFs are briefly discussed. Then two approaches to randomising the modes of the system are considered. The first involves using fixed interface (Craig–Bampton) CMS for the modal analysis, randomising the modes of the component subsystems and using a perturbation to estimate the modal properties of the assembled structure. This is followed by an MCS. In the second approach, an attempt is made to estimate the mode statistics of the structure from the single FEA and then the structure is randomised by taking random samples of these modes in an MCS. Both approaches avoid the need to solve the global eigenvalue problem more than once, and are hence computationally cheap. Finally, numerical examples are presented.

2. Deterministic analysis

2.1. Baseline analysis

The methods used to calculate the EICs for a system are described in detail in Refs. [21,22]. In summary, conventional FEA and modal analysis are used to determine the system's natural frequencies and mode shapes. "Rain-on-the-roof" excitation is applied to each subsystem over a particular frequency band Ω and the energy (strictly twice the kinetic energy) in each subsystem determined. The EIC A_{rs}, which relates the energy in subsystem r per unit power input to subsystem s, is given by

$$A_{rs} = \frac{\sum_j \sum_k \Gamma_{jk} \psi_{jk}^{(r)} \psi_{jk}^{(s)}}{\sum_j \Delta_j \Gamma_{jj} \psi_{jj}^{(r)}}, \tag{8}$$

where the subscripts j and k refer to the jth and kth modes of the system. The cross-modal power

$$\begin{aligned} \Gamma_{jk} &= \frac{1}{\Omega}\int_{\omega\in\Omega} \tfrac{1}{4}\omega^2\beta_{jk}(\omega)\,\mathrm{d}\omega; \\ \beta_{jk} &= \mathrm{Re}\{\alpha_j(\omega)\alpha_k^*(\omega)\}; \\ \alpha_j &= \frac{1}{\omega_j^2-\omega^2+\mathrm{i}\Delta_j\omega} \end{aligned} \tag{9}$$

depends only on the natural frequencies $\omega_{j,k}$ and bandwidths $\Delta_{j,k}$ of modes j and k. Here, Ω is the excitation bandwidth. Broadly, $\Gamma_{jk}\approx 0$ unless both natural frequencies ω_j and ω_k lie in Ω so that both modes are resonant and Γ_{jk} is particularly large if the modes overlap, i.e. they lie in each others bandwidths. The cross-mode participation factor

$$\psi_{jk}^{(r)} = \int_{x\in r} \rho(x)\phi_j(x)\phi_k(x)\,\mathrm{d}x \tag{10}$$

depends only on the mode shapes within subsystem r, $\phi_j(x)$ being the jth mode shape, $\rho(x)$ the mass density and the integral being evaluated only over subsystem r. For a system comprising two subsystems, by inverting the EIC matrix, the apparent CLF $\hat{\eta}_{12}$ is found to be

$$\hat{\eta}_{12} = \frac{1}{\omega}\frac{A_{21}}{A_{11}A_{22}-A_{12}A_{21}}. \tag{11}$$

2.2. Discussion

The EICs and hence the ACLFs depend on the detailed modal properties of the structure: different input data implies different modes and hence different values for the EICs. The situation in general is very complicated, depending on the natural frequencies (through the modal densities and mode spacing statistics) and mode participation factors (which may also be correlated with natural frequencies). However, some general observations can be made.

Averages are taken over a finite frequency band and involve a sampling of N modes, N depending on the modal density. The variance of N depends on the mode spacing statistics (e.g. Poisson, Rayleigh, GOE, etc. [14–20]). The variance of the EICs is then expected to decrease as N^{-1}.

Consider the case of low modal overlap. Now the "self" terms Γ_{jj} dominate the sums, so that only the statistics of the mode participation factors $\psi_{jj}^{(1)}$ are important [22]. Suppose the mean and standard deviation of $\psi_{jj}^{(1)}$ are v_1 and σ_ψ, respectively. For a given number of modes in the band, using statistical results from Ref. [23] it follows that

$$\mathrm{var}[A_{11}] \sim \frac{1}{\Delta^2}\frac{\sigma_\psi^2}{N}\left(1+\frac{\sigma_\psi^2}{v_1^2}\right). \tag{12}$$

For higher modal overlap ($M\sim 1$) the cross-mode terms become important and the situation becomes very complicated, so that the numerical approaches suggested below might be particularly valuable.

The uncertainty in the estimation of the EICs will propagate to the ACLFs during the inversion of the EIC matrix, and the condition number of $\mathbf{A}$ will affect this. Indeed, for small modal overlap the matrix $\mathbf{A}$ can become singular. The form of the variance of ACLF can be estimated by considering the propagation of small errors through the inversion process and the relative variance is of the form

$$\frac{\mathrm{var}\left[\hat{\eta}_{12}\right]}{\eta_{12}^2} \sim \frac{v_1^2 v_2}{N\sigma_\psi^2\left(v_1v_2-\sigma_\psi^2\right)^2}\left(\frac{\eta_{21}+\eta}{\eta}\right). \tag{13}$$

The relative variance is not only dependent on subsystem properties but also on damping loss factor. It is inversely proportional to the number of modes in the band and increases as the damping loss factor decreases.

3. A CMS/perturbational approach to robust estimation

The first approach to robust estimation involves Craig–Bampton (fixed interface) CMS [24]. The steps are summarised here. Each subsystem is modelled individually with the interface fixed using FEA and the component modes calculated. Constraint modes (associated with the interface degrees of freedom (DOFs)) are also included in the model. The individual subsystem models are then assembled. After application of CMS the equations of motion of the structure as a whole can be written in the form [24]

$$\mathbf{M}\ddot{\mathbf{q}} + \mathbf{K}\mathbf{q} = \mathbf{0}, \tag{14}$$

where the vector of DOFs is

$$\mathbf{q} = \begin{Bmatrix} \mathbf{q}_f^{(1)} \\ \mathbf{q}_f^{(2)} \\ \mathbf{q}_c \end{Bmatrix}. \tag{15}$$

Here $\mathbf{q}_f^{(1)}$ and $\mathbf{q}_f^{(2)}$ are the fixed interface modal DOFs of subsystems 1 and 2, respectively (i.e. the modes when the interface is fixed) while $\mathbf{q}_c$ are the constraint mode DOFs (associated with motion of the interface nodal DOFs). The global mass and stiffness matrices are

$$\mathbf{M} = \begin{bmatrix} \mathbf{I} & \mathbf{0} & \mathbf{m}_{fc}^{(1)} \\ \mathbf{0} & \mathbf{I} & \mathbf{m}_{fc}^{(2)} \\ \mathbf{m}_{fc}^{(1)\mathrm{T}} & \mathbf{m}_{fc}^{(2)\mathrm{T}} & \mathbf{m}_{cc} \end{bmatrix}; \quad \mathbf{K} = \begin{bmatrix} \mathrm{diag}(\lambda_j^{(1)}) & \mathbf{0} & \mathbf{0} \\ \mathbf{0} & \mathrm{diag}(\lambda_j^{(2)}) & \mathbf{0} \\ \mathbf{0} & \mathbf{0} & \mathbf{k}_{cc} \end{bmatrix}. \tag{16}$$

The submatrices in Eq. (16) are diagonal matrices of fixed interface eigenvalues for subsystems 1 and 2, $\mathrm{diag}(\lambda_j^{(1,2)})$ (i.e. the natural frequencies squared when the interface is fixed), coupling mass matrices $\mathbf{m}_{fc}^{(1,2)}$ and constraint mass and stiffness matrices $\mathbf{m}_{cc}$ and $\mathbf{k}_{cc}$. The remaining matrices ($\mathbf{I}$ and $\mathbf{0}$) represent the identity matrix and matrices of zeros of appropriate dimension. The global eigenvalue problem (14) is then solved, yielding the global eigenvalues λ_k (squares of the natural frequencies) and mode shapes $\boldsymbol{\phi}_k$ which are in turn used in Eq. (8) to estimate the EICs and the baseline response [6].

Variability is now included in the component modal properties as in the "Local Modal/Perturbational" (LMP) approach of Ref. [12]. A linear perturbation is used to relate the fixed interface eigenvalues and the global modal properties of the structure. For the eigenproblem of Eq. (14), variations $\delta\mu$ in some parameter μ on which $\mathbf{K}$ and $\mathbf{M}$ depend lead to variations in the kth eigenvalue given, to first order, by [25]

$$\delta\lambda_k = \boldsymbol{\phi}_k^{\mathrm{T}} \left[\frac{\partial \mathbf{K}}{\partial \mu} - \lambda_k \frac{\partial \mathbf{M}}{\partial \mu} \right] \boldsymbol{\phi}_k \, \delta\mu, \tag{17}$$

where $\boldsymbol{\phi}_k$ is the kth global eigenvector. Noting the special form of the mass and stiffness matrices in Eq. (16), it follows that a perturbation $\delta\lambda_j^{(i)}$ of the jth fixed interface eigenvalue of subsystem i gives a perturbation

$$\delta\lambda_k = (\phi_k)_j^2 \delta\lambda_j^{(i)} \tag{18}$$

in the kth global eigenvalue, the total perturbation then being

$$\delta\lambda_k = \sum_{i,j} (\phi_k)_j^2 \, \delta\lambda_j^{(i)}. \tag{19}$$

In a similar manner the first-order variation in the kth global eigenvector is [25]

$$\delta\boldsymbol{\phi}_k = \sum_{i,j} \left(\sum_{r \neq k} \frac{(\phi_k)_j (\phi_r)_j}{\lambda_k - \lambda_r} \boldsymbol{\phi}_r \right) \delta\lambda_j^{(i)}. \tag{20}$$

An MCS is now used to estimate the statistics of the global modal properties and hence those of the EICs. The statistics of the fixed interface natural frequencies are assumed and the perturbational relations used to generate the global modes, from which the EICs are calculated. The results of course depend on the standard

deviation σ_g of the global natural frequencies. This must be large enough to sufficiently randomise the system, typically by perturbing out-of-band modes into the analysis band, and in-band modes out of it. Thus, for a bandwidth Ω centred at a frequency ω, the normalised standard deviation for the local modes $\sigma_l \sim \Omega/\omega$.

4. Random sampling of modes

In this section, an alternative approach to randomising the structure is suggested. This involves estimating the statistics of the global modal properties in some way, then taking samples of these modes to generate ensembles of EICs and ACLFs. The statistics can be inferred by general observations, together with specific observations arising from the FEA. First, comments are made concerning some statistics of these modal properties, the natural frequencies and the mode shapes through the self- and cross-mode participation factors $\psi_{jj}^{(r)}$ and $\psi_{jk}^{(r)}$.

4.1. Mode statistics

The EICs depend on the natural frequencies (the modal densities and the mode spacing) and the mode shapes, and hence on their statistics, including any correlation between these quantities. Often, natural frequency spacing has a distribution that is between that of the Gaussian orthogonal ensemble (GOE) or Poisson process depending on the degree of irregularity in the structure. In what follows a brief description of these random processes is given.

4.1.1. Natural frequency spacing statistics: general observations

In Refs. [15,16], the statistics of mode spacing for structures with irregular geometries were seen to asymptote to GOE statistics at high enough frequencies. Similar distributions arise from the eigenvalues of random matrices, under certain conditions [14]. Predictions based on GOE statistics are also seen to agree well with numerical and experimental results [17–20]. On the other hand, structures with symmetries are observed to have spacing statistics with a Poisson distribution [15]. Of course, in practical cases these high-frequency asymptotes might not be applicable, but they provide some guidance as to what distribution might be assumed for the natural frequency spacing statistics.

The probability density function for the GOE [19] is a Rayleigh distribution, i.e.

$$p(x) = \left(\frac{\pi x}{2}\right) e^{-\pi x^2/4}, \tag{21}$$

where x is the spacing normalised by mean spacing (the inverse of the modal density). The distribution is zero at $x = 0$, i.e. it shows level repulsion. Further statistics relate next-nearest-neighbour natural frequencies, etc. For systems with symmetry, mode spacing follows a Poisson distribution for which

$$p(x) = e^{-x}. \tag{22}$$

One would expect variance to depend on spacing statistics and to be higher for Poisson rather than GOE statistics, since the spectrum of the latter is more rigid.

4.1.2. Mode participation factor statistics

The EICs and in turn the CLFs are dependent on both the modal powers and the mode participation factors, which might be correlated. Due to orthogonality of the modes, the cross-mode participation factors are such that $\sum_r \psi_{jk}^{(r)} = \delta_{jk}$. Also the self-terms $\psi_{jj}^{(r)}$ are positive.

It is reasonable perhaps to assume that correlations between mode participation factors are weak and that their variations are small when there are small perturbations in the physical properties: such small perturbations might lead to significant local variations in mode shape, but these are then integrated over the subsystem to find $\psi_{jk}^{(r)}$. It is also reasonable perhaps to assume that correlation between natural frequency spacing and participation factors is unimportant: if two modes are closely spaced then mode repulsion would imply that their participation factors are weakly correlated, while modes whose natural frequencies are not

closely spaced only give significant contributions for large modal overlap, when again such correlation is not important.

Observations from numerical simulations suggest that $\psi_{jj}^{(r)}$ has a bimodal probability distribution. A typical example for the coupled rectangular (RR) plates considered below is shown in Fig. 1a. The locations of the peaks depend on the connection strength of the joint between the subsystems. The reason for this is that each mode tends to be more-or-less localised within one particular subsystem rather than being spread uniformly across the system. Finally, the cross-mode participation factors have zero mean and probability distributions that appear more Gaussian in distribution—an example is shown in Fig. 1b.

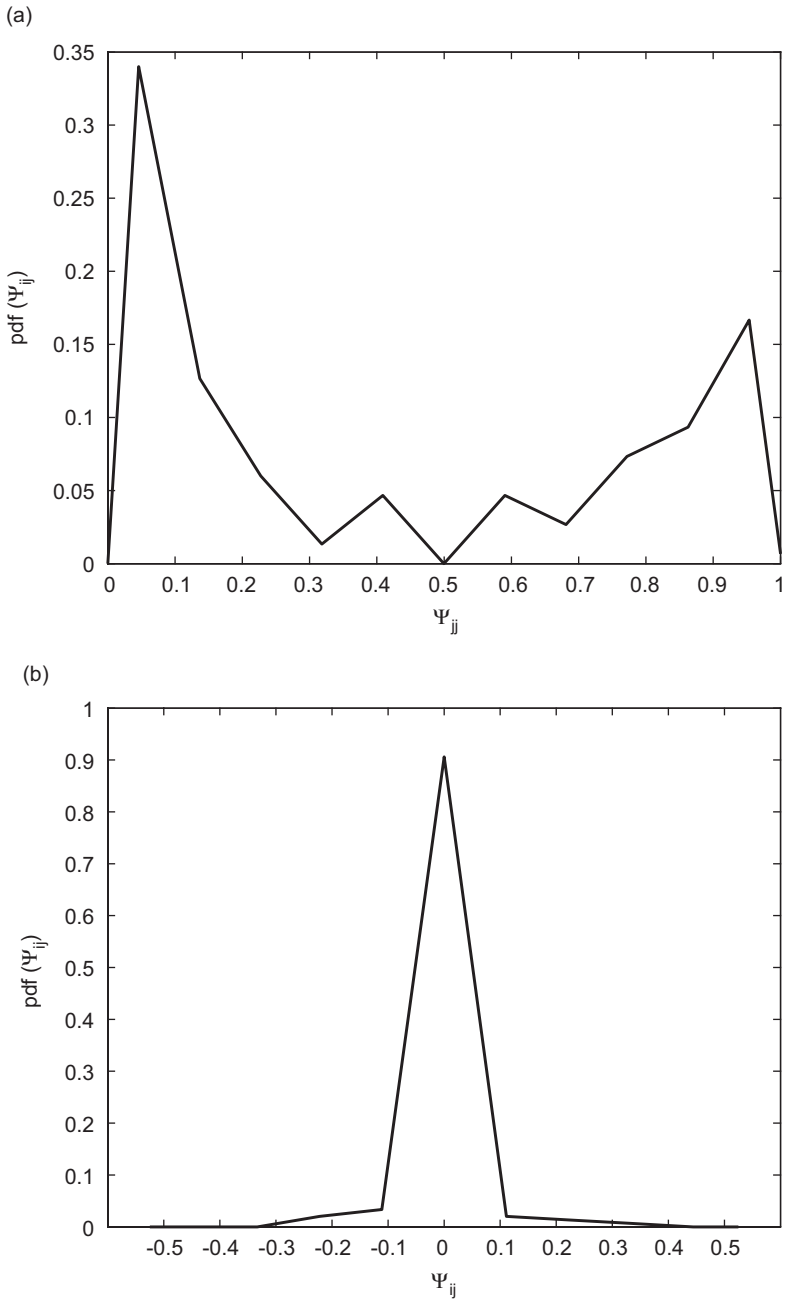

Fig. 1. Probability density functions of participation factors for coupled RR plates: (a) pdf of self-terms $\psi_{jj}^{(r)}$ and (b) pdf of cross-terms $\psi_{j,j+1}^{(r)}$ corresponding to immediate neighbours.

For robust estimation, the system modal properties are randomised once the baseline analysis has been performed. Numerical estimates of EICs are then made from Eq. (8). Two types of system randomisation are suggested below.

4.2. Random selection of centre frequency

The excitation frequency band of interest Ω is selected (e.g. a particular 1/3 octave), the centre frequency being ω_0. It is now assumed that the statistics of the modes of the baseline system over a relatively wide frequency range centred around this band are representative of the statistics of the modes of the ensemble within this band.

An MCS is performed by randomly selecting a frequency ω_c, reasonably close to the actual centre frequency, and taking a frequency band Ω centred on ω_c. The modes within this band Ω are then used to estimate the EICs from Eq. (8). The process is repeated and the results averaged to find robust estimates. The approach is somewhat similar to, but not the same as, averaging over a broader frequency band, since the natural frequencies of the randomly selected modes centred about ω_c are in effect "shifted" by $(\omega_0-\omega_c)$ when processed in Eq. (8). The method requires that the modal statistics (and not the individual modal properties) vary somewhat slowly with frequency. This ensures a good "mixture" of modes, but secular effects (e.g. slow changes in modal density, group velocity, etc., with frequency) will result. It also requires that ω_c be selected from a frequency range which is not so small as to substantially re-use the same modes in each analysis, but not so large as to allow substantial secular effects.

4.3. Random sampling based on estimated probability distributions

In this method of randomisation, the baseline analysis of the system is used to estimate the statistics of natural frequency spacing and mode participation factors. For sampling purposes complete knowledge of the joint probability density function $p(\omega_1,\ldots\omega_n;\psi_{11},\ldots\psi_{nn};\psi_{12},\ldots\psi_{n-1,n};\ldots\psi_{1,n})$ or correlation coefficients and individual probability density functions is, in theory, required. However, the baseline analysis produces a very small sample from which to estimate these statistics. Consequently, certain statistics (e.g. correlations) might be ignored, or *a priori* assumptions made about the probability distributions (e.g. GOE) as discussed in Section 4.1.

The distribution of natural frequencies is dependent on spacing statistics. In the examples below only the immediate neighbour spacing is considered, ignoring the statistics of next-nearest-neighbours. This is expected to only have a minor influence on estimates of the number or distribution of modes in the band and hence the variability of EICs and CLFs, since the modal overlap is necessarily higher when next-nearest neighbour interaction contributes significantly to the EICs. While correlation between mode participation factors was observed, strongly correlated modes do not necessarily happen to be immediate neighbours. This would suggest that for practical purposes this correlation could be ignored. Similarly, although there is some correlation between spacing and cross-mode participation factors, this was seen to be not strong, and the correlation neglected.

For robust estimation, then, an MCS is performed. A set of modes is sampled from the appropriate statistical distribution, some out-of-band modes included and sets of natural frequencies and corresponding participation factors generated. The EICs are estimated, and the process repeated until the MCS sample size is large enough.

5. Numerical examples

In this section numerical examples for systems comprising two edge-coupled plates are presented. The plates are shown in Fig. 2, which are the same as those considered in Ref. [10]. The baseline values of the properties of the plates are given in Table 1. The plates have straight edges and all edges, including the line of coupling, are simply supported. The plates have one of three different shapes, giving three systems whose only difference is the shape of the plates, and hence which have different modes and mode spacing statistics. Both plates are either rectangular (RR), distorted rectangular pentagon (DD) or pentagonal (PP) in shape, giving different

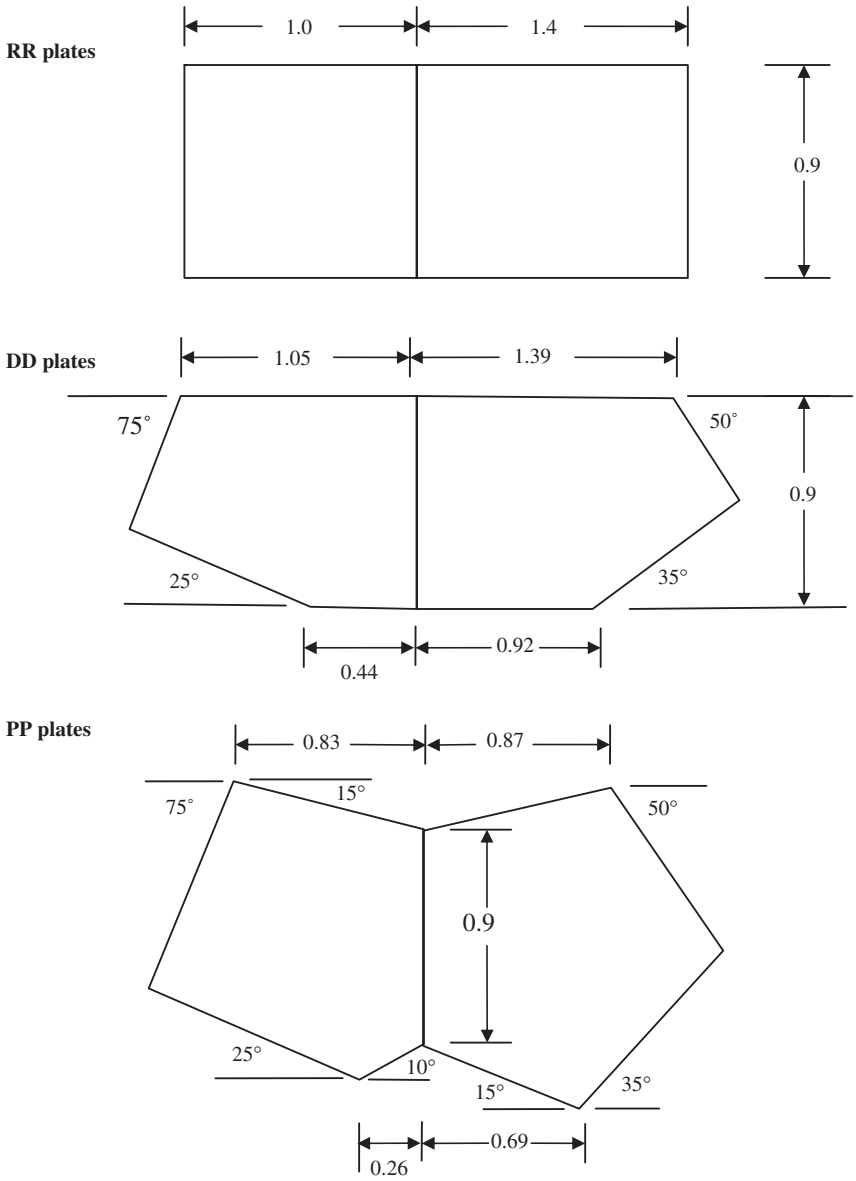

Fig. 2. Coupled plates used in numerical simulations (all dimensions are in m).

Table 1
Physical and geometric properties (SI units) for plates 1 and 2

Elastic modulus	2×10^{11}	Length of coupled edge	0.9
Density	8×10^{3}	Plate area (1, 2)	0.9, 1.26
Poisson's ratio	0.3	Modal density (1, 2)	0.0297, 0.0416
Thickness	0.01	System total modal density	0.0714

amounts of irregularity. ANSYS shell elements of Type 63 were used for the FEA with an element edge length of 0.05 m. Only the DOFs corresponding to flexural motion were retained. 'Rain-on-the-roof' excitation was assumed. The baseline, discrete frequency estimates were made using CMS.

5.1. Baseline structure and results for wide frequency band averages

Fig. 3 shows an example of a transfer mobility (excitation on plate 1, response on plate 2) with $\eta = 0.01$. Below 500 Hz or so the response appears to show distinct resonant behaviour. Above 1500 Hz or so the modal overlap is greater than 1 and individual resonance peaks cannot be clearly seen.

First, EICs and ACLFs were found using averages taken over a wide frequency band (400 Hz, containing approximately 29 modes of the system) with centre frequencies of 500 and 1500 Hz. The ACLFs $\hat{\eta}_{12}$ are shown in Fig. 4 as a function of the modal overlap M of the system as a whole (evaluated at the centre frequency), which was varied by varying the damping loss factor from, typically, 0.0003 to 0.3. This frequency band contains so many modes that the variability in estimates is very small, so that the ACLF approximates the CLF well.

For M less than about 1, $\hat{\eta}_{12} \propto \eta$. The ACLFs are different for the 3 different shaped systems, i.e. they depend on the irregularity of the system, with the PP plates being the more irregular. The 3 ACLFs converge for M larger than about 3, with the PP and DD ACLFs converging at a lower value of M than the regular RR system. For larger M still, the ACLFs asymptote to the (damping-independent) value of CLF predicted by the conventional wave approximation to SEA. Similar behaviour can be seen for the centre frequency of 1500 Hz (Fig. 4b).

Note that the three different shaped systems have the same modal density, the differences arising from the different mode shapes (which tend to be more localised in one plate or the other for the RR system) hence the different values for σ_{ψ}^2, which is largest for the RR system. This explains why the low-M value of the ACLF is smallest for the RR system [22] and is also the cause of the larger variability at low M in ACLFs for the RR system, as will be seen below.

5.1.1. Low and moderate modal overlap approximations for ACLF

At low modal overlap the EICs in Eq. (8) are dominated by the self terms, i.e. those (in the numerator) for which $k = j$. For moderate M, nearest-neighbour mode interactions start to become important (i.e. those terms for which $k = j \pm 1$). Low and moderate M approximations for the EICs, and hence for the ACLFs, can be made by including only these few terms. Fig. 5 shows one example, for which the approximations can be seen to be good for $M < 0.3$ or 0.7 respectively, or thereabouts. One consequence of this is that for low or

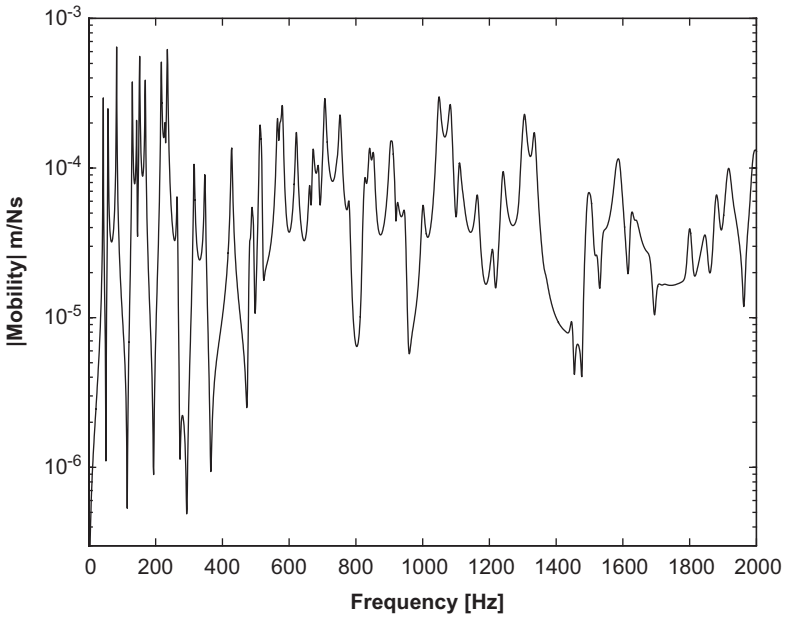

Fig. 3. Example transfer mobility for RR plate.

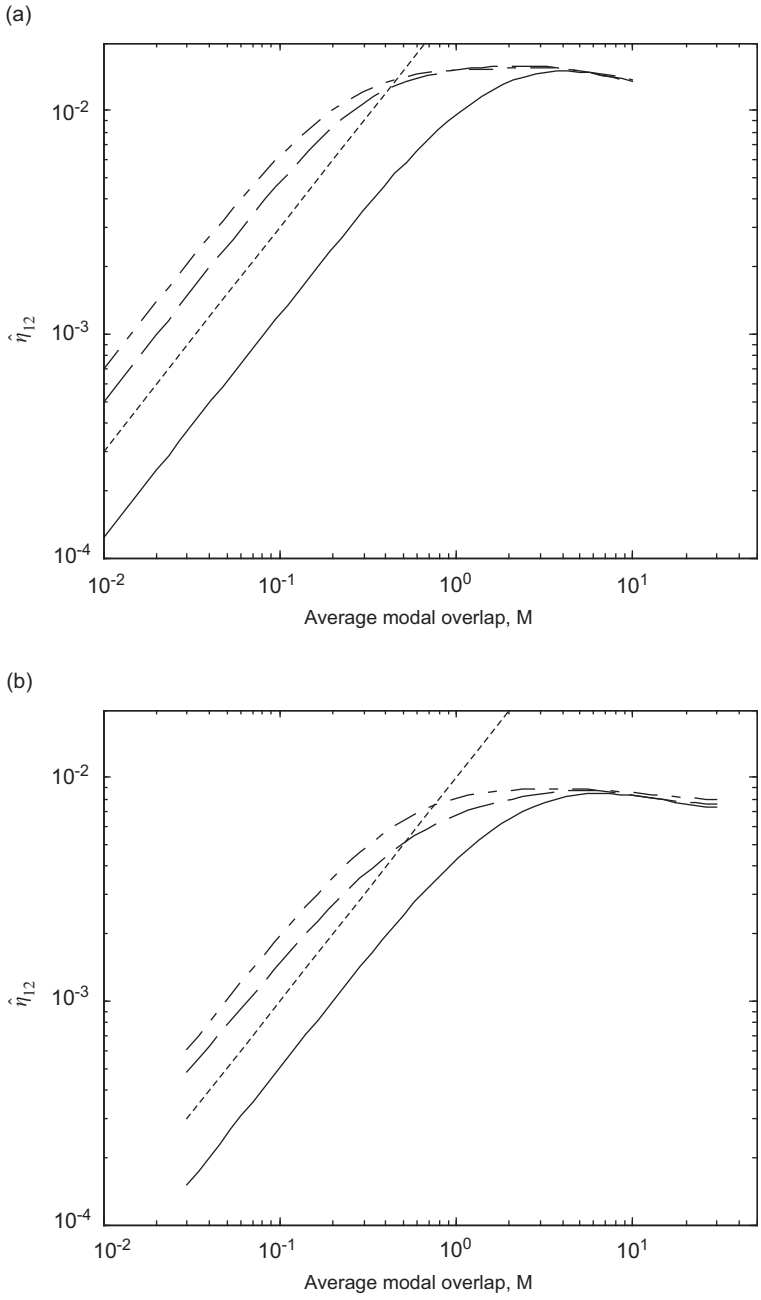

Fig. 4. Variation of apparent coupling loss factor with modal overlap: (a) 500 Hz centre frequency, (b) 1500 Hz centre frequency ——— RR, — — — — DD, · — · — · — · — PP, · · · · · · · · · damping loss factor.

moderate M, when variance is at its largest and robust estimation is more problematical, knowledge of only the statistics of the self-terms and nearest-neighbours is required.

5.2. ACLF statistics from the CMS/perturbational approach: numerical results

In this approach, described in Section 3, a linear perturbation is used to relate changes in the local eigenvalues and the global modal properties, the perturbed eigenvectors are mass normalised, the EIC matrix,

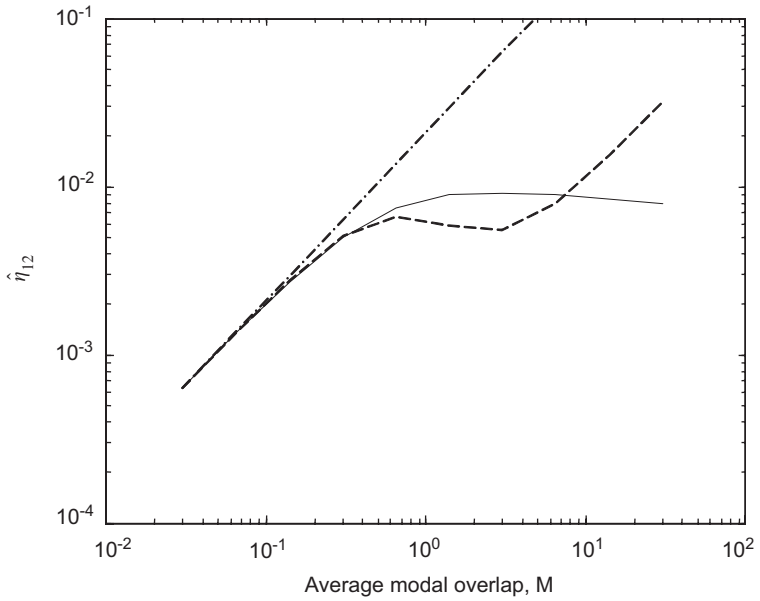

Fig. 5. Apparent coupling loss factor for PP plates, 1500 Hz centre frequency: ———— apparent coupling loss factor, — — — — moderate and · — · — · — · — low modal overlap approximations.

found by a modal sum, is inverted to estimate ACLFs and an MCS is used to estimate statistics. The CLF is also estimated from the inverse of the ensemble average EICs. This is not the same as the mean of the ACLFs, because of the inversion.

In these simulations, the subsystem natural frequencies are assumed to be independent and normally distributed and the subsystems are assumed to be statistically independent. 3000 samples were used in the MCS.

5.2.1. Convergence of statistics

The results of the MCS depend on the standard deviation assumed for the local natural frequencies. These statistics might converge if the normalised standard deviation $\sigma_l \sim \Omega/\omega$. Fig. 6 shows estimates for the 95 percentile ACLF as a function of σ_l. The estimates are approximately constant if $\sigma_l > \Omega/\omega \approx 7\%$. Henceforth this value will be assumed for the standard deviation in the MCS.

5.2.2. Wide bandwidth statistics

Fig. 7 shows the mean ACLF and confidence limits for a wide excitation bandwidth Ω. The confidence interval is narrow over the whole frequency range. The mean ACLF is almost identical to the CLF (i.e. the estimate drawn from the mean EICs). This is because of the large number of modes within the frequency band.

5.2.3. Effect of number of modes in band on variability

The variability of the ACLFs depends on the number of modes in the band. ACLFs and confidence limits are shown in Fig. 8 for bandwidths of 100 and 50 Hz, for which there were, on average, 8 and 4 modes. Compared to Fig. 7 the confidence interval is somewhat larger for the 100 Hz band, and significantly larger for the 50 Hz band, for which there is also a noticeable difference between the mean ACLF and the CLF for low-to-moderate M. The confidence interval decreases as M increases, as is expected.

Fig. 9 shows the ACLF probability density functions at very low modal overlap (0.03) for a 1500 Hz centre frequency and various bandwidths. The broad 400 Hz band contains many modes and the variance is small even though M is so small. The distribution is almost symmetric about the mean. In earlier studies [7,8], it was concluded that the distribution is only Gaussian-like for larger M, but it appears that this might also be the

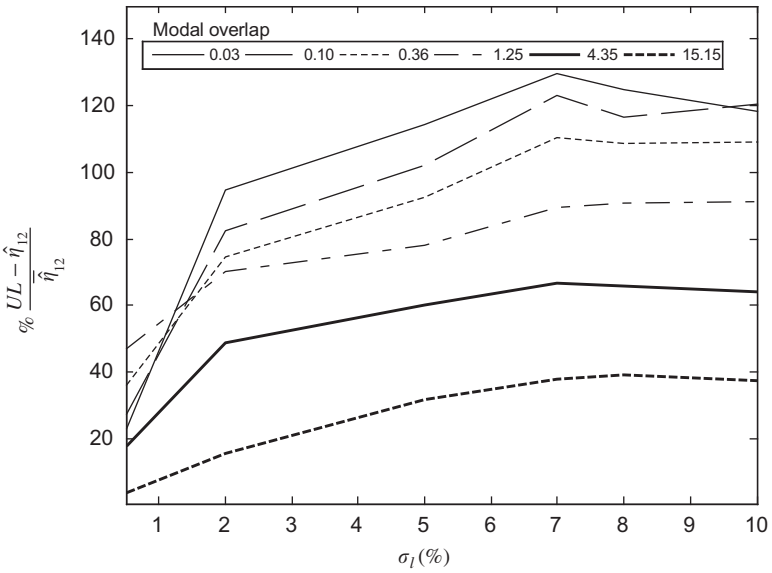

Fig. 6. Convergence of 95 percentile of $\hat{\eta}_{12}$ as a function of normalised standard deviation of local natural frequencies, various modal overlap, RR plates, centre frequency 1500 and 100 Hz bandwidth.

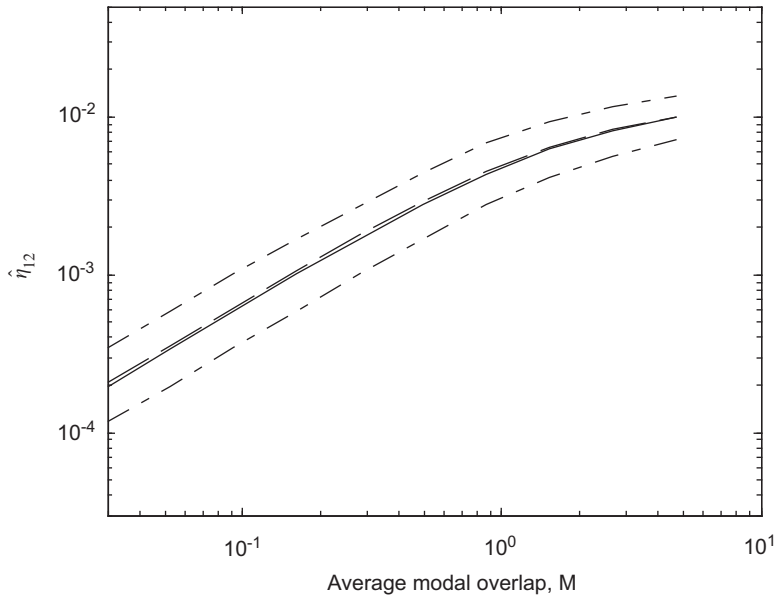

Fig. 7. ACLF $\hat{\eta}_{21}$ for RR plates at 1500 Hz, frequency bandwidth 400 Hz, from CMS/perturbation approach: ——— CLF, — — — mean ACLF, — · — · — 5 and 95 percentile ACLF.

case if there is a sufficient number of modes in the band. The distributions are clearly non-Gaussian for 50 and 100 Hz bandwidths. In part this is because the EIC matrix is poorly conditioned at low M, so that the effects of small deviations from the mean are magnified during the inversion.

5.3. ACLF statistics from random sampling of modes

In Section 4, approaches to randomising the system were suggested by sampling the modal properties in different ways. Fig. 10(a) shows the ACLF and confidence limits estimated by the random centre frequency

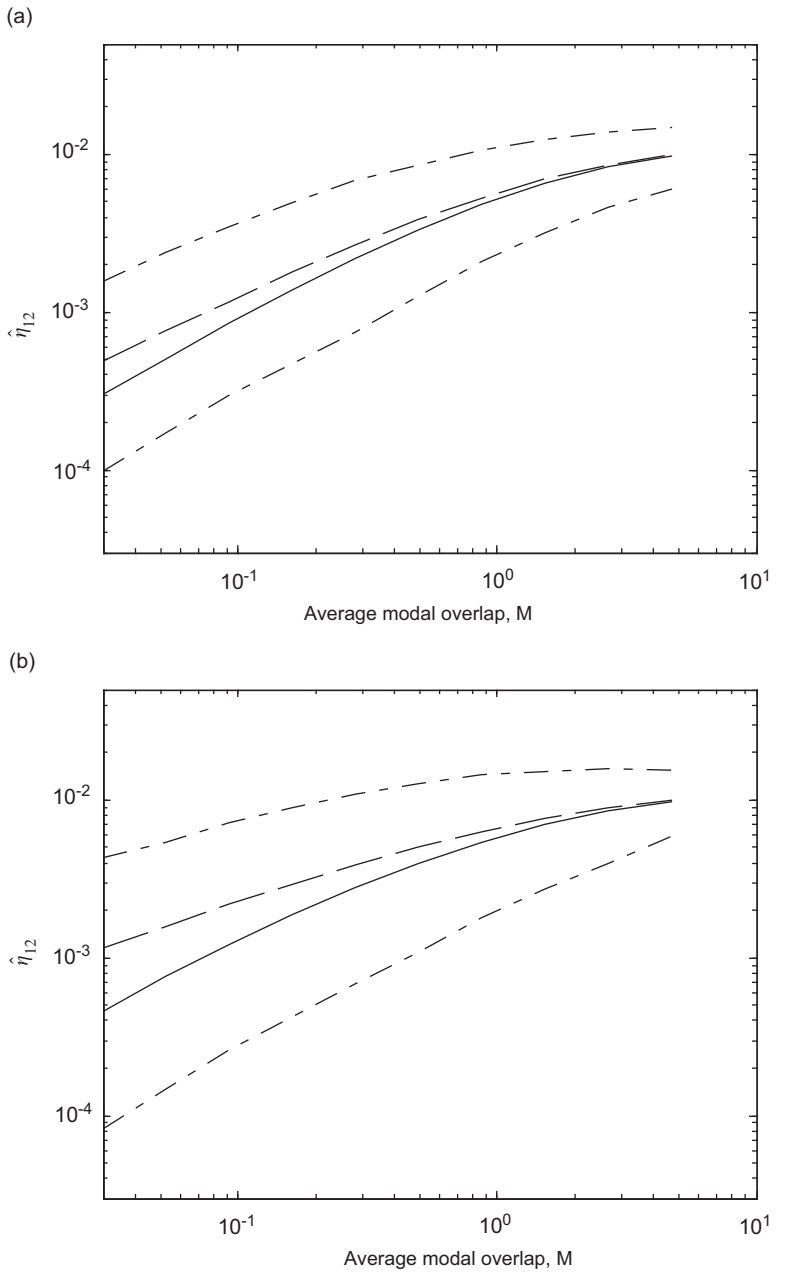

Fig. 8. ACLF $\hat{\eta}_{12}$ for RR plates at 1500 Hz: (a) $\Omega = 100$ Hz and (b) $\Omega = 50$ Hz from perturbation approach: ———— CLF, — — — mean ACLF, — · — · — 5 and 95 percentile ACLF.

selection procedure (in the range from 1185 to 1815 Hz). Again the mean ACLF is somewhat larger than the CLF, the bias in the estimate arising from the skewed probability distribution of the ACLF, with the confidence intervals decreasing as M increases.

The CLF and confidence intervals predicted by the random centre frequency selection approach are very similar to those of the CMS/perturbational approach, although they should not be compared directly, being found from simulations of different random processes.

Fig. 10(b) shows estimates found by first attempting to estimate the full mode statistics (from the properties of the 30 modes closest to the centre frequency). The confidence intervals generated by this method are slightly

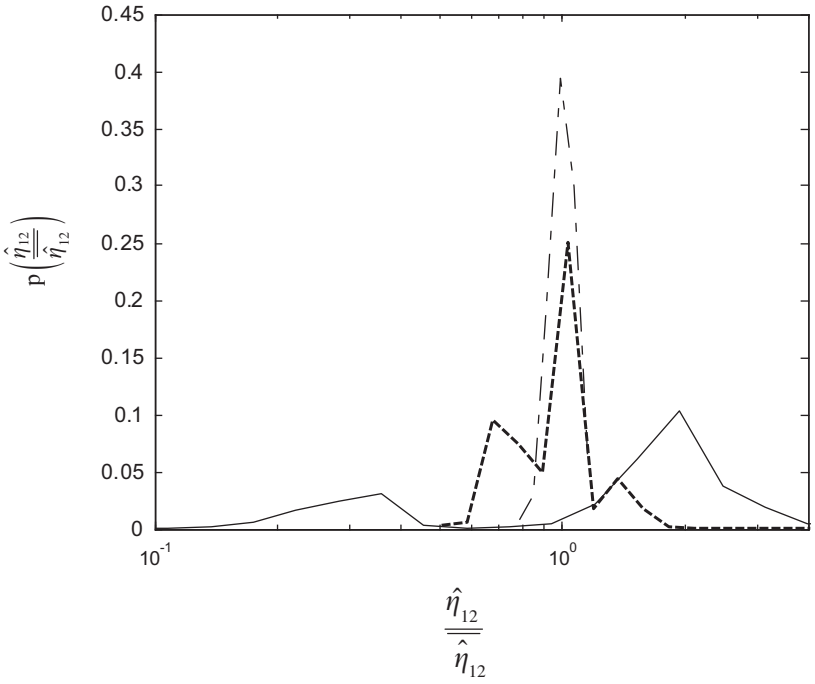

Fig. 9. Probability distribution of apparent coupling loss factors at 1500 Hz and $M = 0.03$: ——— $\Omega = 50$ Hz, — — — $\Omega = 100$ Hz and — · — · — $\Omega = 400$ Hz.

conservative compared with the perturbation and random centre frequency selection approaches (see Figs. 8b and 10a). This may be due to the fact that these statistics are estimated from a relatively small sample of modes (large enough to estimate mean and variance with some confidence, perhaps, but not distributions and correlations).

5.4. Numerical results for various shapes

Fig. 11 shows the ACLFs and confidence limits for DD and PP plates, estimated using the CMS/perturbational method. Comparison with Fig. 8b shows that the confidence interval for (irregular) DD and PP plates is significantly less than that for RR plates. The reasons for this are partly the smaller mode count variance for the irregular systems, together with the smaller variance in self-mode participation factors.

6. Concluding remarks

This paper concerned the estimation of the statistical energy analysis (SEA) coupling loss factors (CLFs) from finite element analysis (FEA). It was noted that a single FEA gives estimates based on a single, selected system, the so-called ACLFs: a different choice of system properties would give different estimates of CLFs. Approaches to robust estimation were discussed. These attempt to give estimates of the SEA-average CLFs that depend less on the details of the chosen system, together with estimates of variance, confidence limits, etc.

Various approaches were described. These involve attempts to randomise the properties of the system being analysed and averaging the resulting estimates, but without repeating the full FEA. The first involves component modal descriptions of the individual subsystems. Perturbations in the subsystem fixed interface natural frequencies can then be related to perturbations in the modal properties of the assembled structure and hence to the energies and CLFs. In the second approach it was assumed that the statistics of the modal properties (natural frequencies and modes shapes) of the system analysed by FEA are a fair representation, when taken over a wide enough frequency range, of the statistics of the modes of the SEA ensemble. The modes of the system are randomly sampled, either by using the properties of modes which lie around

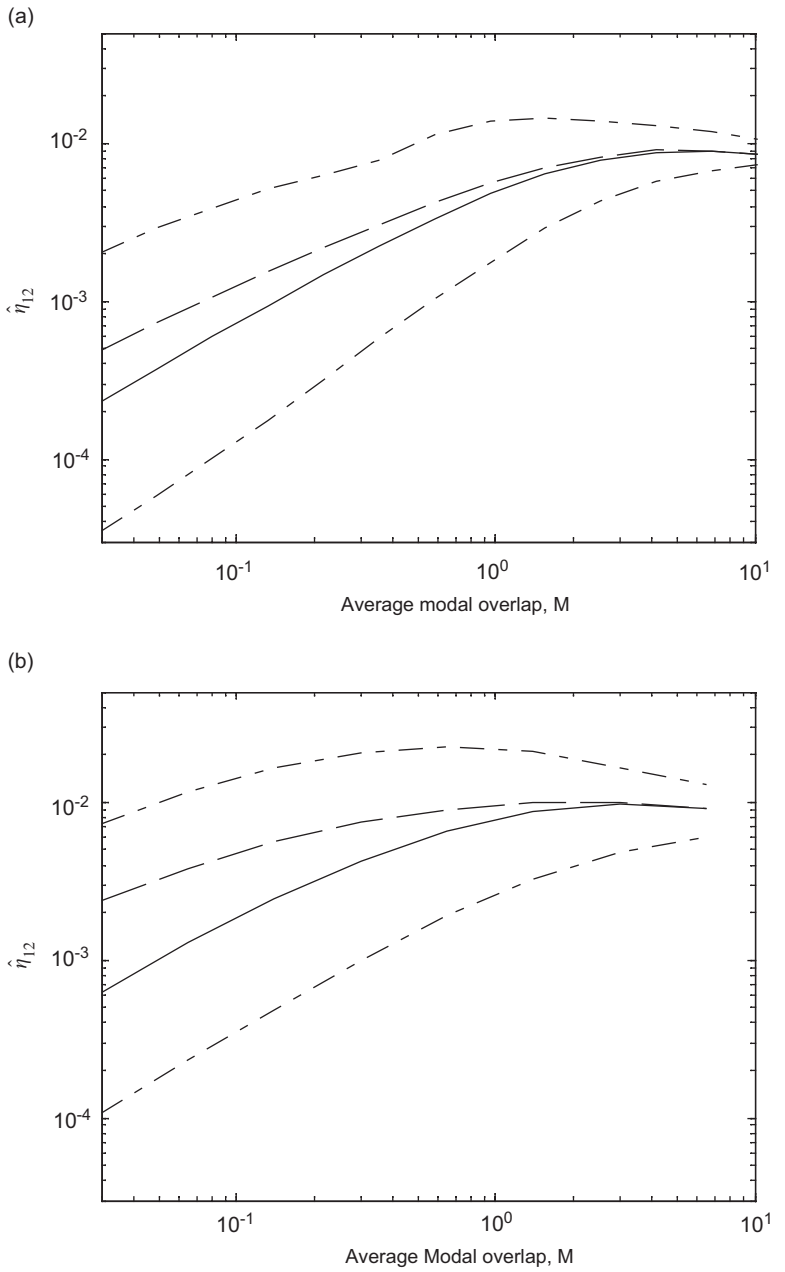

Fig. 10. ACLF $\hat{\eta}_{12}$ for RR plates at 1500 Hz, frequency bandwidth 50 Hz: (a) random centre frequency selection and (b) sampling from probability distribution; ——— CLF, — — — mean ACLF, — · — · — 5 and 95 percentile ACLF.

a randomly selected centre frequency, or by attempting to infer the full modal statistics from the results of the FEA and then sampling from this. These are then followed by a Monte Carlo simulation (MCS) to estimate ACLF statistics. In principle uncertainty in damping can be included straightforwardly, since the modal properties remain unchanged, so that MCS then only involves recalculation of the modal powers and modal sums. Numerical examples were presented. The methods are computationally cheap and in essence post-process the output of a conventional FEA.

While there are of course dangers in drawing conclusions from numerical examples, all methods gave comparable estimates of the CLF, except for very low modal overlap. The variance of the ACLFs generally

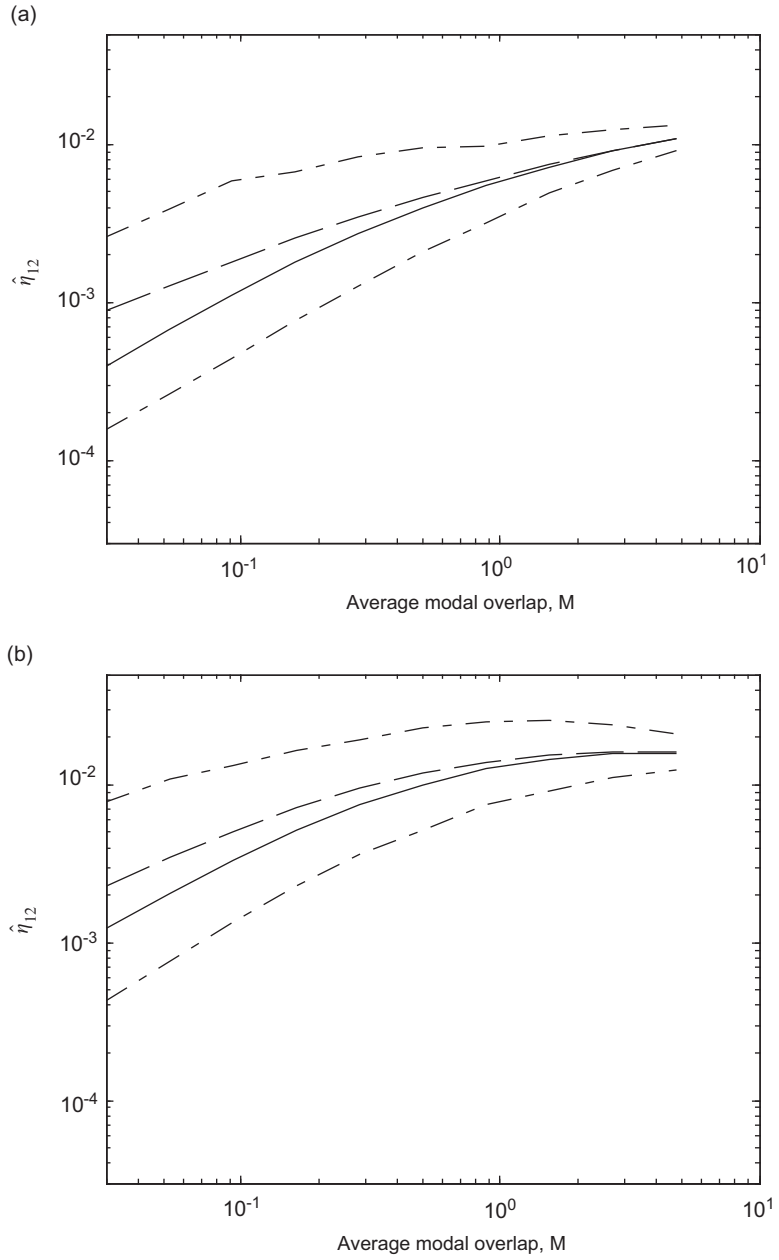

Fig. 11. ACLF $\hat{\eta}_{12}$ at 1500 Hz, frequency bandwidth 50 Hz from CMS/perturbation approach: (a) DD plates and (b) PP plates; ——— CLF, — — — mean ACLF, — · — · — 5 and 95 percentile ACLF.

decreases as modal overlap or the number of modes in the band increase. Variance is also smaller for the irregularly shaped systems. The CMS/perturbational method and the random centre frequency selection method gave comparable estimates of confidence limits, but estimates found by attempting to estimate the full modal statistics are conservative. This is perhaps due to the fact that it is very difficult to accurately estimate the full statistics from such a small sample of modes.

In principle, it is possible to combine the various methods, and perhaps also repeat the FEA a few times, to get a broader range of system properties and responses from which to estimate the statistics. However, this does not avoid the issue of how the ensemble of structures is to be defined in any specific application. In practice this is likely to be case-dependent and problematical. Here, appeal was made to the evidence that

suggests that response statistics are somewhat independent of detailed physical variables if the variability is "large enough" [14–20]. Whether the variability is included in physical properties, component modal properties or system modal properties might therefore be unimportant. In any event, including some randomness is likely to give better estimates of the mean than a single FEA estimate of the ACLFs.

Acknowledgements

The authors gratefully acknowledge the financial support provided by the Leverhulme Trust.

References

[1] R.H. Lyon, R.G. DeJong, *Theory and Applications of Statistical Energy Analysis*, second ed., Butterworth-Heineman, Boston, USA, 1995.
[2] C. Simmons, Structure-borne sound transmission through plate junctions and estimates of SEA coupling loss factors using the FE method, *Journal of Sound and Vibration* 144 (1991) 215–227.
[3] G. Stimpson, N. Lalor, SEA extension of a F.E. model to predict total engine noise, *Internoise* 92 (1992) 557–560.
[4] J.A. Steel, R.J.M. Craik, Statistical energy analysis of structure-borne sound transmission by finite element methods, *Journal of Sound and Vibration* 178 (1993) 553–561.
[5] C.R. Fredö, SEA-like approach for the derivation of energy flow coefficients with a finite element model, *Journal of Sound and Vibration* 199 (1997) 645–666.
[6] B.R. Mace, P.J. Shorter, Energy flow models from finite element analysis, *Journal of Sound and Vibration* 233 (2000) 369–389.
[7] D.A. Bies, S. Hamid, In situ determination of loss and coupling loss factors by the power injection method, *Journal of Sound and Vibration* 70 (1980) 187–204.
[8] F.J. Fahy, A.D. Mohammed, A study of uncertainty in applications of SEA to coupled beam and plate systems—part 1: computational experiments, *Journal of Sound and Vibration* 158 (1992) 45–67.
[9] F.F. Yap, J. Woodhouse, Investigation of damping effects on statistical energy analysis of coupled structures, *Journal of Sound and Vibration* 197 (1997) 351–371.
[10] B.R. Mace, J. Rosenberg, The SEA of two coupled plate: an investigation into the effects of subsystem irregularity, *Journal of Sound and Vibration* 212 (1998) 395–415.
[11] C. Hopkins, Statistical energy analysis of coupled plate systems with low modal density and low modal overlap, *Journal of Sound and Vibration* 251 (2001) 193–214.
[12] B.R. Mace, P.J. Shorter, A local modal/perturbational method for estimating frequency response statistics of built-up structures with uncertain parameters, *Journal of Sound and Vibration* 242 (2001) 793–811.
[13] A.N. Thite, B.R. Mace, Robust estimation of coupling loss factors from finite element analysis, *ISVR Technical Memorandum*, No. 935, University of Southampton, 2004.
[14] M.L. Mehta, *Random Matrices*, Academic Press, New York, 1991.
[15] R.L. Weaver, Spectral statistics in elastodynamics, *Journal of Acoustical Society of America* 85 (3) (1989) 1005–1013.
[16] P. Bertelsen, C. Ellegaard, E. Hugues, Distribution of eigenfrequencies for vibrating plates, *The European Physical Journal B* 15 (2000) 87–96.
[17] R.S. Langley, V. Cotoni, Response variance prediction in the statistical energy analysis of built-up systems, *Journal of Acoustical Society of America* 115 (2004) 706–718.
[18] R.S. Langley, A.W.M. Brown, The ensemble statistics of the energy of a random system subjected to harmonic excitation, *Journal of Sound and Vibration* 275 (2004) 823–846.
[19] R.S. Langley, A.W.M. Brown, The ensemble statistics of the band-averaged energy of a random system, *Journal of Sound and Vibration* 275 (2004) 847–857.
[20] V. Cotoni, R.S. Langley, M.R.F. Kidner, Numerical and experimental validation of variance prediction in the statistical energy analysis of built-up systems, *Journal of Sound and Vibration* 288 (2005) 701–728.
[21] B.R. Mace, Statistical energy analysis, energy distribution models and system modes, *Journal of Sound and Vibration* 264 (2003) 391–409.
[22] B.R. Mace, Statistical energy analysis: coupling loss factors, indirect coupling and system modes, *Journal of Sound and Vibration* 279 (2005) 141–170.
[23] J.S. Bendat, A.G. Piersol, *Random Data: Analysis and Measurement Procedures*, Wiley, New York, 2000.
[24] R.R. Craig, *An Introduction to Computer Methods*, Wiley, New York, 1981.
[25] R.L. Fox, M.P. Kapoor, Rates of change of eigenvalues and eigenvectors, *AIAA Journal* 6 (1968) 2426–2429.